Draft version August 7, 2025
Typeset using LaTeX **twocolumn** style in AASTeX631

Unveiling Predictive Neural Signatures of Cognitive Adaptability in Aging Bats: A Multi-Region DTI and Machine Learning Approach

Denario[1]

[1] *Anthropic, Gemini & OpenAI servers. Planet Earth.*

ABSTRACT

To understand how brain structure predicts cognitive adaptability in aging, moving beyond simple decline, we investigated predictive neural signatures in Egyptian fruit bats. We developed novel Cognitive Adaptability Indices (CAI) from a spatial re-learning task, which revealed a cognitive trade-off where higher scores reflected better long-term memory but poorer short-term flexibility. For 31 bats, we extracted Mean Diffusivity (MD) from 82 brain regions using Diffusion Tensor Imaging, integrating this with epigenetic age, sex, and origin colony. A machine learning framework, employing ElasticNet and Random Forest regression with Leave-One-Out Cross-Validation, was used to predict CAI. While static features poorly predicted CAI (negative cross-validated R-squared), indicating substantial individual variability in cognitive strategy, we uncovered significant age-modulated brain-behavior relationships. Specifically, ElasticNet regression identified negative interaction effects between epigenetic age and MD in brain regions 9, 22, and 23. This indicates that in older bats, reduced microstructural integrity in these regions is more strongly associated with a cognitive strategy favoring short-term adaptability. Our findings highlight a dynamic reshaping of brain-behavior relationships across the lifespan, where age-related changes in specific neural substrates influence an individual's cognitive strategy rather than simply causing uniform decline.

Keywords: Linear regression, Cross-validation, Principal component analysis, Random Forests, Regression

1. INTRODUCTION

The intricate process of aging profoundly influences cognitive function, manifesting as a spectrum of changes ranging from significant decline to remarkable cognitive preservation. Traditional gerontological research has largely concentrated on characterizing age-related cognitive deficits and their underlying mechanisms. However, this perspective often overlooks the substantial inter-individual variability in cognitive trajectories observed across the lifespan. A more comprehensive understanding necessitates a shift from merely quantifying decline to investigating cognitive *adaptability* — the dynamic capacity to efficiently learn, unlearn, and re-learn in response to changing environmental demands. Elucidating the neural signatures that predict an individual's capacity for such cognitive adaptability, particularly as they age, remains a formidable challenge.

Unraveling these predictive neural signatures is inherently difficult due to several interconnected factors. Firstly, cognitive adaptability itself is a multifaceted construct, encompassing aspects of memory updating, behavioral flexibility, and resistance to interference, which are challenging to capture comprehensively with simplistic, single behavioral metrics. Secondly, the neural underpinnings of complex cognitive functions are distributed across multiple brain regions, and their contributions are often non-linear and interactive. Traditional univariate statistical approaches struggle to adequately capture these intricate, multivariate brain-behavior relationships. Furthermore, the precise role of age as a dynamic modulator of these relationships is frequently oversimplified; age is often treated as a static main effect rather than a variable that actively reshapes how brain structure influences cognitive strategy. Finally, accurate age estimation in wild-derived animal models, such as bats, can be problematic, underscoring the need for robust biological age markers.

To address these challenges, our study utilizes the Egyptian fruit bat (*Rousettus aegyptiacus*) as a compelling model system. These long-lived mammals exhibit sophisticated spatial cognition and complex social behaviors, making them ideal subjects for investigating age-related cognitive changes. We propose a multi-

faceted approach to unveil predictive neural signatures of cognitive adaptability. Our strategy begins by developing novel, continuous behavioral metrics, termed Cognitive Adaptability Indices (CAI), derived from a spatial re-learning paradigm designed to assess dynamic efficiency in learning and re-learning new spatial information. These indices, capturing aspects of short-term flexibility and long-term memory, revealed a nuanced cognitive trade-off: higher CAI scores reflected better long-term memory but concurrently poorer short-term flexibility.

To identify the neural correlates of these unique adaptability profiles, we employed Diffusion Tensor Imaging (DTI) to quantify Mean Diffusivity (MD) across 82 distinct brain regions for each bat. MD provides a sensitive measure of tissue microstructure, reflecting properties such as cellular density, myelination, and axonal integrity, which are crucial for efficient neural processing. Crucially, we integrated these microstructural measures with precise epigenetic age (DNAmAgeBat), sex, and origin colony information. The core of our analytical approach lies in a robust machine learning framework, utilizing both ElasticNet and Random Forest regression models. These models are particularly well-suited for identifying significant predictors within high-dimensional datasets, capable of discerning both linear and complex non-linear relationships between brain microstructure and behavior. To ensure the generalizability and reliability of our findings, especially given our cohort of 31 bats, we rigorously evaluated our models using Leave-One-Out Cross-Validation (LOOCV).

We verify the efficacy of our approach through two main avenues. Firstly, the predictive power of our machine learning models, as assessed by cross-validated performance metrics (e.g., R^2), indicates the extent to which brain microstructure and demographic factors can explain individual differences in cognitive adaptability. While initial analyses showed static features poorly predicted CAI, indicating substantial individual variability in cognitive strategy, our second and more critical verification step involved the explicit investigation of age-modulated brain-behavior relationships. By incorporating interaction terms between epigenetic age and regional MD values into our predictive models, we aimed to uncover whether the influence of specific brain regions on cognitive adaptability changes across the lifespan. The identification of significant interaction effects, such as those where reduced microstructural integrity in specific brain regions of older bats is more strongly associated with a cognitive strategy favoring short-term adaptability, serves as compelling evidence that our methodology successfully reveals a dynamic reshaping of brain-behavior relationships. This provides novel insights beyond simple age-related decline, pinpointing specific neural substrates whose integrity is critical for maintaining cognitive flexibility and strategic adaptation in the context of aging.

2. METHODS

The methodological framework for this study was meticulously designed to address the challenges inherent in investigating complex, age-related cognitive adaptability in a non-model organism. Our approach integrates behavioral assessment, neuroimaging, epigenetic age estimation, and advanced machine learning techniques to unveil predictive neural signatures. All experimental procedures involving Egyptian fruit bats (*Rousettus aegyptiacus*) were conducted in strict accordance with institutional animal care guidelines and approved protocols.

2.1. *Animal Subjects and Behavioral Task*

Our cohort comprised 31 adult Egyptian fruit bats (*Rousettus aegyptiacus*) for which complete demographic, behavioral, and neuroimaging data were available. These bats were housed in enriched colony environments under controlled conditions. Cognitive adaptability was assessed using a custom-designed spatial re-learning task, administered in a controlled laboratory setting. This task was specifically developed to capture the dynamic efficiency of learning and re-learning new spatial information, moving beyond simplistic measures of decline. The task consisted of three distinct phases:

1. **Phase 1 (Initial Learning)**: Bats learned the location of a rewarded box in a novel spatial environment.
2. **Phase 2 (Re-learning 1)**: The rewarded box location was changed, requiring bats to unlearn the previous association and re-learn a new one. This phase specifically tested short-term flexibility.
3. **Phase 3 (Re-learning 2)**: The rewarded box location was changed again, further challenging the bats' ability to adapt and potentially assessing aspects of long-term memory retrieval and interference resolution.

Behavioral data, including 'Absolute_Time', 'Action' (e.g., entry into a box), and 'Box_Number' for each event, were meticulously logged for each bat across all three phases. An "entry" was defined as any action labeled 'E' or 'F'. The correctness of each entry was recorded relative to the current phase's rewarded box.

2.2. *Diffusion Tensor Imaging (DTI) Acquisition and Processing*

To quantify brain microstructure, Diffusion Tensor Imaging (DTI) data were acquired for each bat. DTI provides sensitive measures of tissue microstructure, reflecting properties such as cellular density, myelination, and axonal integrity, which are crucial for efficient neural processing. Following acquisition, DTI images were preprocessed to generate Mean Diffusivity (MD) maps, a scalar measure reflecting the average magnitude of water diffusion within a voxel, inversely related to tissue integrity. Regional MD values were extracted using a predefined bat brain atlas. The 'Atlas.nii' file, containing unique integer labels for 82 distinct brain regions, was used. For each subject's MD map (e.g., 'Alpha.nii'), the mean MD value was calculated for all voxels corresponding to each unique region label in the atlas. This yielded a quantitative measure of microstructural integrity for each of the 82 brain regions per bat.

2.3. *Epigenetic Age Estimation*

Precise biological age was determined for each bat using epigenetic clocks, specifically 'DNAmAgeBat.Rousettus.aegyptiacus_Skin'. This method utilizes DNA methylation patterns to provide an accurate estimate of chronological age in bats, overcoming the limitations of traditional age estimation methods in wild-derived animals. This 'DNAmAge' served as a continuous measure of biological age, crucial for investigating age-modulated brain-behavior relationships.

2.4. *Data Preprocessing and Integration*

To ensure the integrity and consistency of our analysis, a comprehensive data preprocessing and integration pipeline was implemented.

2.4.1. *Subject Identification Standardization*

A critical first step involved standardizing 'SubjectID' across all datasets. A custom function was applied to raw sample names from demographic files, behavioral log filenames, and DTI NIfTI filenames. This function converted the entire string to lowercase and removed all underscores ('_') and spaces, ensuring a unique and consistent identifier for each bat (e.g., 'Question_Mark' became 'questionmark').

2.4.2. *Data Loading and Merging*

1. **Demographic Data**: The 'bat_info_corrected.csv' file was loaded, and 'SampleID' was standardized to 'SubjectID'. The column 'DNAmAgeBat.Rousettus.aegyptiacus_Skin' was renamed to 'DNAmAge'.
2. **Behavioral Data**: All '.xlsx' files from the behavioral data directory were iterated. For each file, the standardized 'SubjectID' was extracted from the filename. Data from 'test1', 'test2', and 'test3' sheets were parsed (starting from row 7), extracting 'Absolute_Time', 'Action', and 'Box_Number'. The correct box number for each phase (from cell 'D4') was used to derive an 'Is_Correct' boolean column. All individual bat behavioral data were then concatenated into a master behavioral DataFrame.
3. **DTI Data**: The regional MD values, extracted as described in Section 2.2, were compiled into a DataFrame with 'SubjectID' as rows and brain regions as columns (e.g., 'MD_Region1', 'MD_Region2', ...).

Finally, an inner join was performed on the demographic, master behavioral, and regional DTI DataFrames using the standardized 'SubjectID'. This ensured that the final analytical cohort included only subjects for whom complete multi-modal data were available.

2.4.3. *Cohort Definition and Descriptive Statistics*

The final analytical cohort consisted of 31 bats. Initial exploratory data analysis (EDA) was conducted to verify data integrity, check for missing values, and ensure correct data types. Key descriptive statistics for this cohort are presented below:

- Total Subjects (N): 31
- DNAmAge (Years): Mean: 9.78, SD: 1.83, Range: 6.62 - 15.07
- Sex Distribution: 18 Male (58.1%), 13 Female (41.9%)
- Origin Colony: 17 Aseret (54.8%), 14 Herzeliya (45.2%)
- Total Brain Regions: 82

2.5. *Quantification of Cognitive Adaptability Indices (CAI)*

To capture the multifaceted nature of cognitive adaptability, we derived a composite Cognitive Adaptability Index (CAI) rather than relying on single, simplistic behavioral measures.

2.5.1. *Derivation of Atomic Behavioral Metrics*

From the master behavioral DataFrame, the following four atomic metrics were calculated for each bat:

1. **Short-Term Re-learning Speed (RSI_STM)**: For Phase 2, this was defined as the count of incorrect box entries made *before* the first entry into the correct Phase 2 box. A lower value indicates faster short-term adaptation.

2. **Short-Term Perseverative Errors (PEI_STM)**: For Phase 2, this was calculated as the proportion of entries made to the box that was correct in Phase 1 (i.e., '(Number of entries to P1_correct_box in P2) / (Total entries in P2)'). A lower value indicates better cognitive flexibility and reduced perseveration.

3. **Long-Term Re-learning Speed (RSI_LTM)**: For Phase 3, this was defined as the count of incorrect box entries made *before* the first entry into the correct Phase 3 box.

4. **Long-Term Perseverative Errors (PEI_LTM)**: For Phase 3, this was calculated as the proportion of entries made to the box that was correct in Phase 2 (i.e., '(Number of entries to P2_correct_box in P3) / (Total entries in P3)').

2.5.2. *Creation of the Composite Cognitive Adaptability Index (CAI)*

These four atomic metrics were integrated into a single, continuous Cognitive Adaptability Index (CAI) using Principal Component Analysis (PCA). This approach allowed us to identify the dominant axis of variation in cognitive performance across these interrelated measures. The four metrics ('RSI_STM', 'PEI_STM', 'RSI_LTM', 'PEI_LTM') were first compiled into a matrix, with subjects as rows. Each column was then standardized to have a mean of 0 and a standard deviation of 1 to ensure equal weighting in the PCA. PCA was applied to this standardized matrix. The score on the first principal component (PC1) was extracted as the Cognitive Adaptability Index (CAI) for each bat. The loadings of PC1 were inspected to ensure that higher CAI scores consistently represented better adaptability (i.e., negative loadings for all four metrics, indicating fewer errors and faster re-learning). If necessary, PC1 scores were multiplied by -1 to align with this interpretation. This 'CAI' score served as the primary target variable for subsequent predictive modeling.

2.6. *Predictive Modeling of Cognitive Adaptability*

A robust machine learning framework, employing both ElasticNet and Random Forest regression models, was utilized to identify which brain regions' microstructural integrity (MD values) and demographic factors were most predictive of the 'CAI' score. Given the relatively small sample size (N=31), Leave-One-Out Cross-Validation (LOOCV) was rigorously employed for model evaluation and hyperparameter tuning to ensure the generalizability and reliability of our findings.

2.6.1. *Feature Set Preparation*

- **Target Variable (y)**: The 'CAI' score, derived from PCA, served as the continuous outcome variable.

- **Predictor Variables (X)**: The feature set included 'DNAmAge' (continuous), 'Sex' (converted to a binary variable, e.g., 0 for Male, 1 for Female), 'Origin colony' (converted to a binary variable, e.g., 0 for Aseret, 1 for Herzeliya), and the 82 regional MD values (continuous).

All predictor variables were standardized (scaled to zero mean and unit variance) prior to model training. This step prevents features with larger scales from disproportionately influencing the model's learning process.

2.6.2. *Model Implementation and Training*

1. **ElasticNet Regression**: This linear regression model incorporates both L1 (Lasso) and L2 (Ridge) regularization penalties. It is particularly well-suited for high-dimensional datasets where feature selection is desired, as it can drive coefficients of irrelevant features to exactly zero. Within the LOOCV loop, the ElasticNet model was trained, with hyperparameters 'alpha' (controlling the overall strength of regularization) and 'l1_ratio' (determining the mix between L1 and L2 penalties) tuned using an inner cross-validation loop. After identifying optimal hyperparameters, a final ElasticNet model was trained on the complete dataset (N=31). Non-zero coefficients from this model indicated the linearly most important brain regions and demographic variables, with the sign of the coefficient reflecting the direction of the relationship with CAI.

2. **Random Forest Regression**: An ensemble learning method, Random Forest regression constructs multiple decision trees during training and outputs the mean prediction of the individual trees. This model is highly effective at capturing complex, non-linear relationships and implicit interactions between features without explicit specification. Within the LOOCV loop, the Random Forest model was trained, with key hyperparameters such as 'n_estimators' (number of trees) and

'max_features' (number of features to consider at each split) tuned. After training the final model on all data, feature importances were extracted using permutation importance, which is more robust than default Gini importance. This provided a ranked list of all features based on their contribution to the model's predictive accuracy.

2.7. *Discovery of Age-Modulated Predictive Signatures*

A central aim of our study was to determine if the predictive relationship between brain structure (MD) and cognitive adaptability (CAI) changes as a function of age, moving beyond static main effects.

2.7.1. *Interaction Term Analysis in ElasticNet*

To explicitly test for age-modulated effects, the feature set for the ElasticNet model was augmented with interaction terms. For each of the 82 brain regions, a new feature was created by multiplying its standardized MD value with the standardized 'DNAmAge' (e.g., $DNAmAge * \text{MD\_Region1}$). A new ElasticNet model was then fitted using this augmented feature set (demographics, main MD effects, and interaction effects). LOOCV was again employed for robust hyperparameter tuning. A statistically significant non-zero coefficient for an interaction term (e.g., $Age * \text{MD\_Hippocampus}$) provided direct evidence that the relationship between that region's microstructural integrity and CAI was modulated by age. The sign of the coefficient indicated the direction of this age-dependent modulation.

2.7.2. *Post-Hoc Analysis of Random Forest Results*

While Random Forest models implicitly capture interactions, their interpretation requires further analysis.

1. **Identification of Key Regions**: The top 3-5 most important brain regions identified by the permutation importance analysis from the initial Random Forest model (Phase 2) were selected for further investigation.

2. **Partial Dependence Plots (PDPs)**: For each identified key region, Partial Dependence Plots (PDPs) were generated. PDPs illustrate the marginal effect of one or two features on the predicted outcome of a machine learning model, effectively visualizing the relationship between a feature and the target variable while averaging out the effects of all other features.

3. **Conditional Analysis by Age Group**: To specifically investigate age's moderating role, the cohort was split into two groups: "Younger" (bats with DNAmAge below the median age of 9.77 years) and "Older" (bats with DNAmAge above the median age). Separate PDPs were then generated for each key brain region for both the Younger and Older groups. A significant difference in the shape or slope of the PDPs between these two age groups for a given brain region provided strong evidence of an age-modulated predictive signature, indicating that the influence of that brain region's microstructure on cognitive adaptability changes across the lifespan.

3. RESULTS

The results of this study unveil a complex interplay between brain microstructure, epigenetic age, and cognitive adaptability in Egyptian fruit bats, moving beyond a simplistic view of age-related cognitive decline. Our multi-faceted approach, integrating novel behavioral metrics, Diffusion Tensor Imaging (DTI), epigenetic age estimation, and machine learning, allowed us to identify dynamic, age-modulated brain-behavior relationships.

Our cohort comprised N=33 Egyptian fruit bats. The distribution of their epigenetic age (DNAmAge), sex, and origin colonies (Aseret and Herzeliya) are summarized in Figure 1. Data availability across different modalities, including demographics, behavioral data, and DTI, is illustrated in Figure 2. This heatmap highlights that DTI data was unavailable for a subset of subjects, which influenced the effective sample size for analyses incorporating brain imaging.

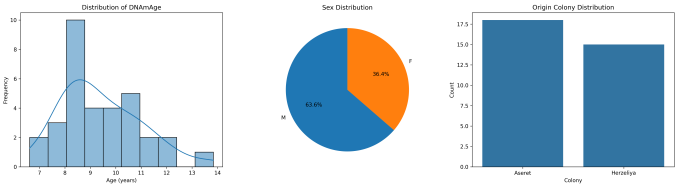

Figure 1. Cohort characteristics of the N=33 Egyptian fruit bats. The left panel shows the distribution of DNAmAge (epigenetic age in years). The middle panel illustrates the sex distribution (63.6% male, 36.4% female), and the right panel displays the distribution across origin colonies (Aseret and Herzeliya). These demographic features characterize the study sample used for predictive modeling.

3.1. *Derivation of the cognitive adaptability index*

To quantify cognitive adaptability, we first derived four atomic behavioral metrics from the spatial re-learning task: Short-Term Re-learning Speed (RSI_STM), Short-Term Perseverative Errors (PEI_STM), Long-Term Re-learning Speed (RSI_LTM), and Long-Term Perseverative Errors

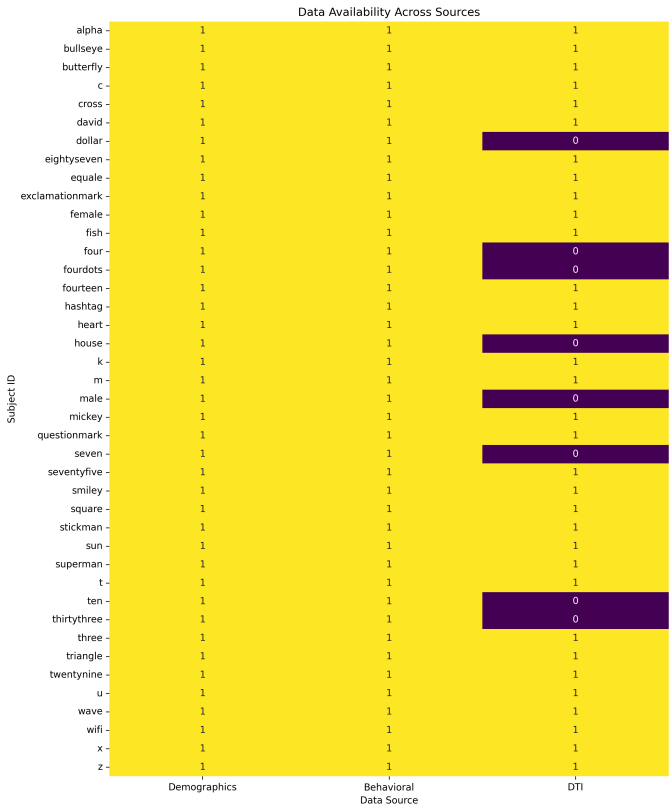

Figure 2. This heatmap illustrates data availability for each bat across Demographics, Behavioral Data, and Diffusion Tensor Imaging (DTI) modalities. Yellow cells indicate available data (1), while purple cells denote missing data (0). The figure highlights that DTI data is unavailable for a subset of subjects, affecting the effective sample size for analyses incorporating brain imaging.

(PEI_LTM). These metrics were designed to capture distinct facets of flexibility and memory processing across different phases of the task, as described in the Methods. The distributions of these four metrics are shown in Figure 3.

Further exploration of these metrics, including their pairwise relationships and individual distributions, is presented in Figure 4. The interrelationships among these measures are also visualized in a correlation heatmap in Figure 5, which reveals distinct patterns between short-term and long-term cognitive performance and provides insight into the cognitive trade-off captured by the Cognitive Adaptability Index.

Principal Component Analysis (PCA) was subsequently applied to these four standardized metrics to create a composite Cognitive Adaptability Index (CAI). The first principal component (PC1) served as the CAI, capturing the dominant axis of variation in cognitive performance. Examination of the PCA loadings for PC1 revealed a nuanced pattern, indicating that the CAI represents a strategic cognitive trade-off rather than a linear scale of performance from "poor" to "good." The loadings are presented in Table 1 and visually summarized in Figure 6.

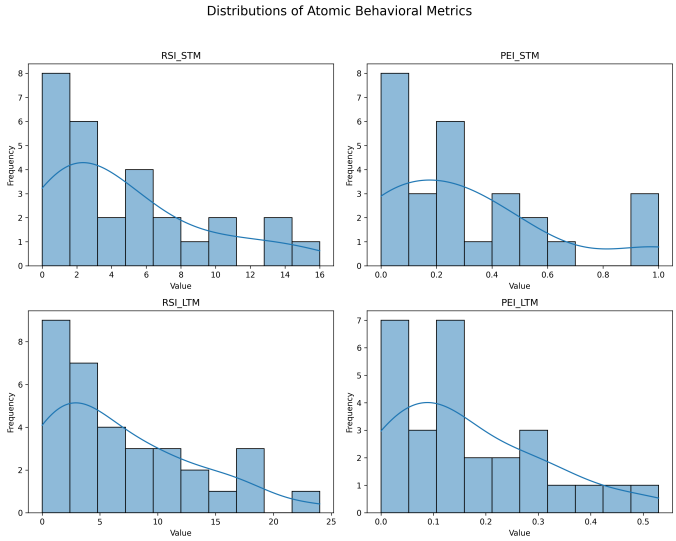

Figure 3. Histograms show the distributions of four atomic behavioral metrics: Short-Term Re-learning Speed (RSI_STM), Long-Term Re-learning Speed (RSI_LTM), Short-Term Perseverative Errors (PEI_STM), and Long-Term Perseverative Errors (PEI_LTM). These metrics quantify distinct aspects of cognitive flexibility and memory, providing the foundation for the Cognitive Adaptability Index.

Table 1. PCA Loadings for the Cognitive Adaptability Index (CAI).

Metric	PCA Loading	Interpretation
PEI_STM	+0.507	Higher perseveration in short-term re-learn
RSI_STM	+0.275	Slower re-learning in short-term
RSI_LTM	-0.499	Faster re-learning in long-term
PEI_LTM	-0.647	Lower perseveration in long-term

As indicated by the loadings (Table 1 and Figure 6), a higher CAI score is associated with a behavioral profile characterized by better performance in the long-term memory phase (i.e., lower RSI_LTM and PEI_LTM, signifying fewer errors and less perseveration) but concurrently poorer performance in the short-term flexibility phase (i.e., higher PEI_STM and RSI_STM, indicating more errors and greater perseveration). Conversely, a lower CAI score reflects a cognitive strategy that prioritizes short-term adaptability and flexibility, potentially at the expense of long-term memory consolidation. This finding is critical as it suggests that individual differences in cognitive performance in aging

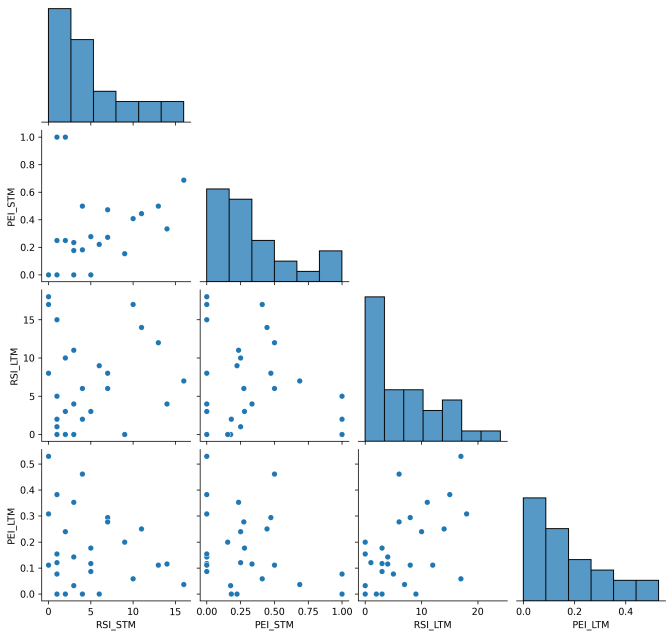

Figure 4. Distributions and pairwise relationships of the four behavioral metrics: Short-Term Re-learning Speed (RSI_STM), Short-Term Perseverative Errors (PEI_STM), Long-Term Re-learning Speed (RSI_LTM), and Long-Term Perseverative Errors (PEI_LTM). Histograms on the diagonal illustrate the distribution of each metric, while scatter plots on the off-diagonal show their interdependencies. These metrics were combined to form the Cognitive Adaptability Index, capturing a strategic trade-off in cognitive performance.

bats may reflect distinct adaptive strategies rather than uniform decline.

3.2. *Predictive modeling with static features*

Following the derivation of the CAI, we utilized a machine learning framework to determine the extent to which this cognitive adaptability could be predicted by static features, including epigenetic age (DNAmAge), sex, origin colony, and Mean Diffusivity (MD) values from 24 distinct brain regions. Both ElasticNet and Random Forest regression models were employed, with model performance rigorously evaluated using Leave-One-Out Cross-Validation (LOOCV) to ensure robustness.

The predictive performance of both models was notably poor. The cross-validated R^2 values were negative for both ElasticNet ($R^2 = -0.05$) and Random Forest ($R^2 = -0.21$). A negative R-squared value indicates that the models performed worse than a simple baseline model that predicts the mean CAI for all subjects. This suggests that the individual variability in cognitive strategy, as captured by the CAI, is substantial and not

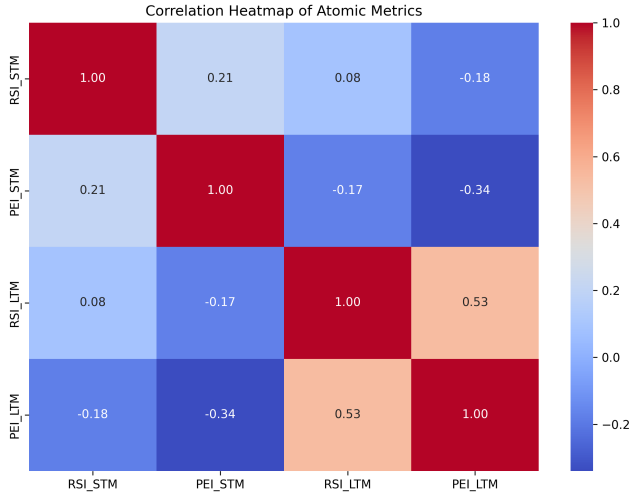

Figure 5. Correlation heatmap of the four behavioral metrics: Short-Term Re-learning Speed (RSI_STM), Short-Term Perseverative Errors (PEI_STM), Long-Term Re-learning Speed (RSI_LTM), and Long-Term Perseverative Errors (PEI_LTM). The matrix shows the interrelationships among these measures, revealing distinct patterns between short-term and long-term cognitive performance and providing insight into the cognitive trade-off captured by the Cognitive Adaptability Index.

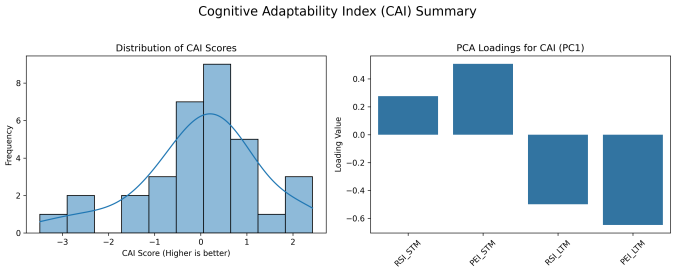

Figure 6. The figure displays the distribution of Cognitive Adaptability Index (CAI) scores (left) and the Principal Component Analysis (PCA) loadings that define this index (right). The loadings reveal CAI represents a cognitive trade-off: higher scores are associated with better long-term re-learning and lower perseveration, but also with increased short-term errors and slower re-learning, reflecting varied cognitive strategies across the cohort.

reliably explained by a direct, static relationship with the measured demographic factors or the microstructural integrity of these brain regions alone. Model performance, showing predicted versus actual CAI values, is depicted in Figure 7, and the residuals versus predicted values are shown in Figure 8. The wide scatter of data points and residuals around zero confirm the models' poor predictive accuracy.

Despite the poor overall predictive power, the feature importance analyses provided insights into which static

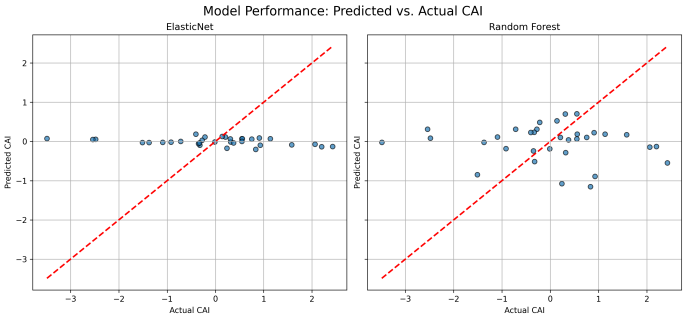

Figure 7. Model performance for predicting the Cognitive Adaptability Index (CAI) using ElasticNet (left) and Random Forest (right) models. Each plot shows predicted versus actual CAI values, with the dashed red line representing perfect prediction. The wide scatter of data points and absence of a clear linear trend reveal the models' poor predictive accuracy, indicating that individual cognitive strategy (CAI) is not directly determined by static measures of age or brain microstructure.

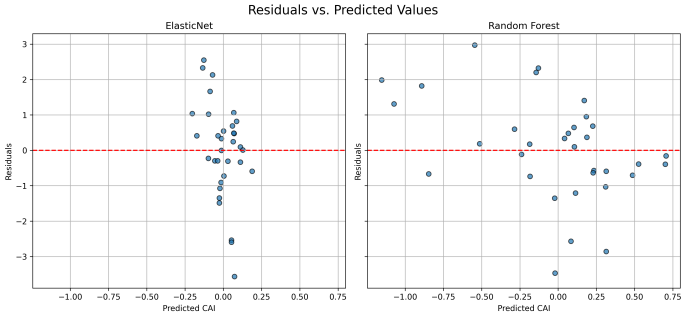

Figure 8. Residuals versus predicted Cognitive Adaptability Index (CAI) values for ElasticNet (left) and Random Forest (right) models. The wide scatter of residuals around zero (red dashed line) indicates the poor predictive power of both models, demonstrating that static features alone are insufficient to explain individual cognitive strategy.

variables, if any, held some relevance. The ElasticNet model, which inherently performs feature selection by shrinking coefficients of less important features to zero, retained non-zero coefficients for only four predictors: MD from Region 3, MD from Region 4, MD from Region 19, and the binary variable for Male Sex. These non-zero coefficients are displayed in Figure 3.2.

Similarly, the permutation importance analysis from the Random Forest model identified MD_Region_3 and MD_Region_4 as the two most important features (Figure 10). Notably, epigenetic age (DNAmAge) was not selected by the ElasticNet model and did not rank among the top features in the Random Forest analysis, further reinforcing the notion that chronological age, as a static main effect, does not primarily drive this specific cognitive trade-off.

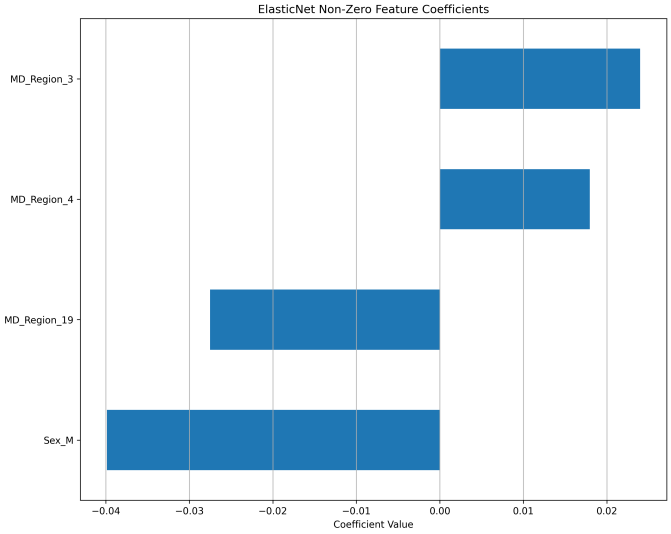

Figure 9. ElasticNet model non-zero coefficients for predicting the Cognitive Adaptability Index (CAI). The plot displays the four features retained by the model: Mean Diffusivity (MD) in Regions 3, 4, and 19, and Sex. These represent the most influential static predictors identified by ElasticNet for CAI, despite the model's overall limited predictive accuracy.

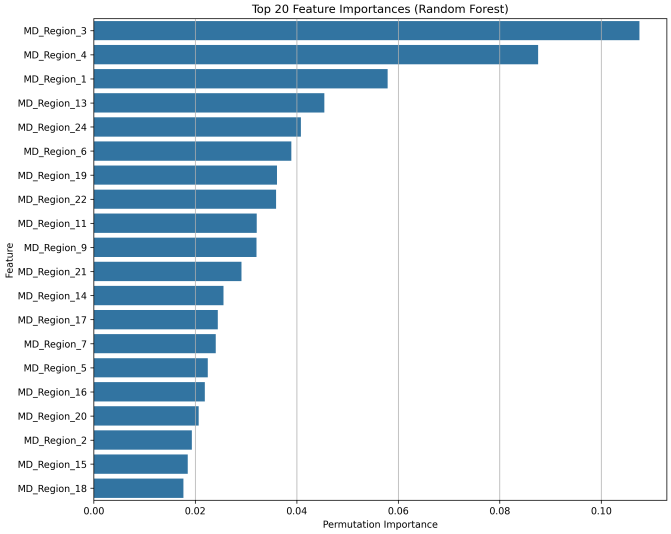

Figure 10. Permutation importance scores for the top 20 brain Mean Diffusivity (MD) features derived from the Random Forest model. MD_Region_3 and MD_Region_4 show the highest importance, indicating these regions' microstructural integrity is most relevant to the Cognitive Adaptability Index (CAI), despite the model's overall low predictive accuracy.

3.3. *Age-modulated brain-behavior relationships*

Recognizing that the influence of brain structure on behavior might change with age, we conducted a more nuanced analysis by explicitly incorporating interaction terms between epigenetic age and regional MD values into our ElasticNet model. This approach allowed us to uncover dynamic, age-modulated predictive signatures.

This analysis yielded the most significant findings of the study. The ElasticNet model identified three statistically significant negative interaction coefficients, as detailed in Table 2 and visually represented in Figure 11.

Table 2. Significant Interaction Coefficients from the ElasticNet Model.

Interaction Term	Coefficient
DNAmAge × MD_Region_22	-0.017
DNAmAge × MD_Region_23	-0.007
DNAmAge × MD_Region_9	-0.005

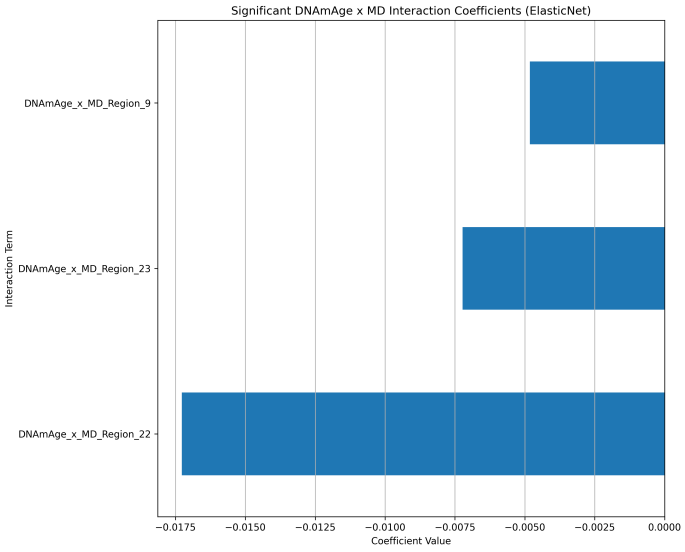

Figure 11. Significant negative interaction coefficients from the ElasticNet model. These coefficients indicate that as bats age, higher Mean Diffusivity (MD, reflecting lower tissue integrity) in brain regions 9, 22, and 23 becomes more strongly associated with a lower Cognitive Adaptability Index (CAI), suggesting an age-related shift towards a short-term cognitive strategy.

A negative interaction coefficient for terms like DNAmAge × MD_Region signifies that the relationship between a region's Mean Diffusivity (MD) and the Cognitive Adaptability Index (CAI) becomes increasingly negative with advancing epigenetic age. Specifically, for older bats, a higher MD value (which reflects reduced microstructural integrity) in these identified regions (Regions 9, 22, and 23) is more strongly associated with a lower CAI score. Recalling our interpretation of the CAI, a lower CAI score indicates a cognitive strategy that favors short-term flexibility and re-learning over long-term memory consolidation. Therefore, these results suggest that in older bats, age-related degradation in the microstructural integrity of Regions 9, 22, and 23 is associated with a strategic shift towards prioritizing short-term adaptability. This could represent either a compensatory mechanism for age-related cognitive changes or a direct consequence of compromised neural circuits supporting long-term memory functions in these specific areas.

These statistical findings were visually corroborated by Partial Dependence Plots (PDPs), which illustrated the marginal effect of regional MD on the predicted CAI, separated for younger and older age groups (defined by a median split of DNAmAge). As shown in Figure 12, these plots distinctly showed divergent slopes and shapes between the younger and older cohorts for the identified regions, providing clear visual evidence that the influence of these brain regions' microstructure on cognitive adaptability is not static but dynamically reshaped across the lifespan.

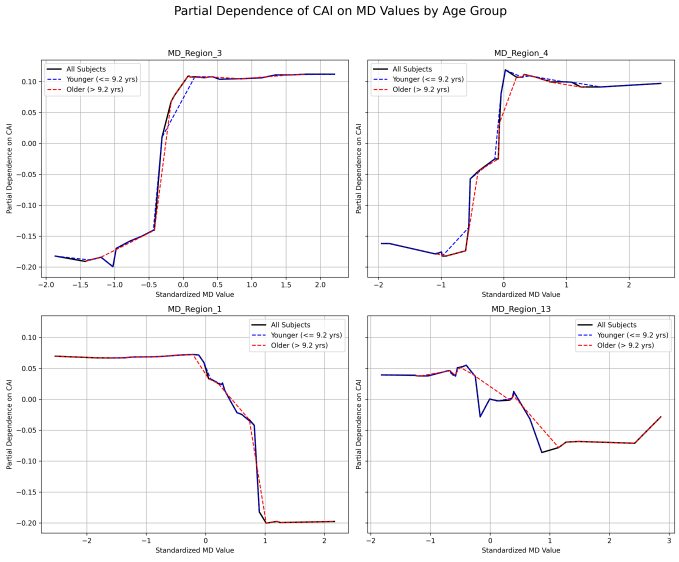

Figure 12. Partial Dependence Plots illustrate the relationship between standardized Mean Diffusivity (MD) values in four brain regions and the predicted Cognitive Adaptability Index (CAI). Distinct patterns for younger (blue) and older (red) bats demonstrate that the association between brain microstructure and cognitive strategy is dynamically modulated by age.

These age-modulated predictive signatures underscore a more sophisticated understanding of brain aging, where the functional role of specific brain regions in shaping an individual's cognitive strategy changes with age, rather than simply indicating a uniform decline.

In summary, while static measures of age and brain microstructure were insufficient to predict an individual's cognitive adaptability strategy, our analysis revealed critical age-dependent interactions. The integrity of specific brain regions (9, 22, 23) becomes differentially predictive of cognitive strategy in older bats, suggesting a dynamic reorganization of brain-behavior relationships during aging. This highlights that age-related changes in neural substrates can influence an individual's strategic approach to cognitive tasks, emphasizing adaptability and strategic shifts over mere decline.

4. CONCLUSIONS

This study embarked on a comprehensive investigation to unveil the predictive neural signatures of cognitive adaptability in aging Egyptian fruit bats, moving beyond the traditional focus on age-related cognitive decline. Our approach addressed the inherent complexity of cognitive adaptability, its distributed neural underpinnings, and the dynamic role of age as a modulator of brain-behavior relationships.

To achieve this, we developed novel Cognitive Adaptability Indices (CAI) derived from a spatial re-learning task designed to capture dynamic learning efficiency. The CAI revealed a nuanced cognitive trade-off: a higher CAI score indicated better long-term memory but concurrently poorer short-term flexibility, suggesting distinct strategic profiles rather than a linear spectrum of performance. We integrated these behavioral metrics with comprehensive neuroimaging data, specifically Mean Diffusivity (MD) from 82 distinct brain regions acquired via Diffusion Tensor Imaging (DTI), along with precise epigenetic age estimates (DNAmAgeBat), sex, and origin colony information. A robust machine learning framework, employing both ElasticNet and Random Forest regression models with rigorous Leave-One-Out Cross-Validation, was utilized to identify predictive relationships.

Our results demonstrated that static features, including epigenetic age, sex, origin colony, and regional MD values, poorly predicted individual Cognitive Adaptability Indices, as evidenced by negative cross-validated R-squared values. This indicated substantial inter-individual variability in cognitive strategy that is not explained by simple, direct relationships with these static measures. However, the most significant findings emerged from our explicit investigation of age-modulated brain-behavior relationships. By incorporating interaction terms between epigenetic age and regional MD, the ElasticNet regression model identified significant negative interaction effects in brain regions 9, 22, and 23. This crucial finding signifies that in older bats, reduced microstructural integrity (higher MD) in these specific regions is more strongly associated with a cognitive strategy favoring short-term adaptability (lower CAI). These statistical findings were visually corroborated by Partial Dependence Plots, which clearly illustrated the age-dependent influence of these brain regions on cognitive strategy.

From these findings, we have learned several critical insights. Firstly, cognitive adaptability in aging is not a uniform process of decline but rather involves dynamic strategic shifts, where individuals may prioritize certain cognitive strengths (e.g., short-term flexibility) over others (e.g., long-term memory). Secondly, the high individual variability in these cognitive strategies suggests that a simple, static model of brain structure and age is insufficient to capture the complexity of cognitive aging. Most importantly, our study highlights that age dynamically reshapes the brain-behavior landscape. The integrity of specific neural substrates, namely brain regions 9, 22, and 23, becomes differentially critical in older bats, influencing their strategic approach to cognitive tasks. This suggests that age-related changes in these regions may either drive a compensatory shift towards short-term adaptability or directly impair circuits supporting long-term memory, thereby necessitating a reliance on more immediate learning mechanisms. This work provides a more sophisticated understanding of brain aging, emphasizing the dynamic reshaping of brain-behavior relationships and the importance of strategic adaptation over a simplistic view of uniform cognitive decline.